Large Dispersive Effects near the Band Edges of Photonic Crystals

Arnout Imhof, Willem L. Vos, Rudolf Sprik, and Ad Lagendijk

Van der Waals-Zeeman Instituut, Universiteit van Amsterdam, NL-1018 XE Amsterdam, The Netherlands
(Received 23 March 1999)

We have used phase-sensitive ultrashort-pulse interferometry to study the modification of optical pulse propagation near the photonic band edges in colloidal crystals consisting of polystyrene spheres in water. A strong suppression of the group velocity is found at frequencies near the L gap of the fcc lattice. The group velocity dispersion diverges at the band edges and shows branches of both normal dispersion and anomalous dispersion, which can be interpreted as large changes in the effective mass, both positive and negative. We obtain excellent agreement with the dynamical diffraction theory.

The propagation of electromagnetic radiation in three-dimensional (3D) periodic dielectric structures is strongly modified if the wavelength of the radiation is on the order of the lattice spacing. Such structures are called photonic crystals [1]. Their periodicity gives rise to photonic band structures in a way that is analogous to electronic band structures. Frequencies for which there are no corresponding wave vectors for propagation in a given direction are in the stop gap. These waves satisfy the Bragg condition and will be diffracted. Much of the recent interest in photonic crystals stems from the possibility of making lattices for which there exists a range of frequencies in which waves cannot propagate in any direction in the crystal [1–3]. Such a photonic band gap occurs when the coupling between light and lattice is sufficiently strong. This has thus far not been accomplished for optical wavelengths. If a lattice could be constructed with a photonic band gap at optical frequencies this would result in spectacular effects such as the inhibition of spontaneous emission [2] and localization of light [3].

Experimental investigations of the propagation of light in photonic crystals have largely been limited to measurements of transmission [4–7] or reflection spectra [8]. Two interferometric experiments have been done which measured small changes in the phase velocity in photonic crystals [9,10]. While these techniques are very useful to determine the presence of stop gaps they do not provide full information on the light propagation through the crystal. Time-resolved experiments are essential to reveal the dynamics of the electromagnetic fields in the photonic crystal. In one-dimensional (1D) multilayer systems, pulsed-laser experiments have demonstrated extremely short tunneling times at in-gap frequencies [11,12], as well as very low group velocities at near-gap frequencies [13]. Pulse slowing was also seen in a synthetic opal [14]. For three-dimensional crystals, fascinating predictions have been made of dynamical effects such as localized photon states [3] and nonlinear interactions leading to optical bistability [6], gap solitons [15], and optical limiting and switching [16].

In this Letter, we present time-resolved measurements of a three-dimensional optical photonic crystal. Phase-sensitive ultrashort-pulse interferometry [17] is used to probe the modification of light propagation close to the band edges of a colloidal crystal, where the dispersion relation $\omega(k)$ between frequency ω and wave vector k of a propagating wave becomes nonlinear. The time-resolved experiments enable direct and independent measurements of the group velocity $v_g = d\omega/dk$ of a pulse and of the group velocity dispersion (GVD), quantified by the parameter $\beta_2 = d^2k/d\omega^2$, of the same pulse. The GVD can be interpreted as being inversely proportional to an effective photon mass, in analogy to electronic band structures. This property has never been measured in photonic crystals. We find strong divergences in both the pulse delay and the GVD at frequencies near the stop gap at the L point of the face-centered cubic lattice, in excellent agreement with the dynamical diffraction theory [18]. Such behavior has not even been observed before in one-dimensional systems, where pulse delays are seen to oscillate just outside the gap and to be small and nearly constant inside it [19] due to the small number of repeating units. Because the diverging quantities are associated with the band edges, measurements such as these will become an important tool in accurately characterizing the band gaps. This is critical for determining whether or not a candidate crystal possesses a photonic band gap.

The photonic crystals consisted of deionized suspensions of polystyrene spheres in water. The sphere diameter was 222 nm. Suspensions of volume fraction 20% were put in flat glass capillaries with a path length of 0.4 mm. Some crushed beads of ion exchange resin were also added. The negatively charged spheres ordered into a face-centered cubic lattice with the (111) planes parallel to the glass surface, as shown by x-ray diffraction [20]. The diffraction angles of wavelengths in the tuning range of our laser are close to 180°. Because of gravitational compaction, the lattice constant varies slightly with the height in the capillary. Therefore, all measurements were done on the same position.

Phase-sensitive time-resolved interferometry [17] was used to study pulse transmission through the photonic crystals. This technique measures the interferometric cross correlation function of a laser pulse transmitted by

the sample with the incoming pulse. We used bandwidth-limited ultrashort pulses (70–100 fs) from a Ti:sapphire laser (Spectra Physics Tsunami), tunable from 720 to 835 nm, with a repetition rate of 82 MHz. First, a double-pulsed signal is obtained with a Mach-Zehnder inter-ferometer in which the reference arm is empty and the sample arm contains the sample. A sample area of 1 mm was illuminated at normal incidence. The power inci-dent upon the sample was ~0.1 W, low enough to avoid nonlinear optical effects. The sample capillary was index matched in a 1 cm optical glass cuvette filled with glyc-erol to avoid refraction by the capillary. The sample and reference beams emerging from the interferometer were carefully overlapped. This produced a pair of pulses: an undisturbed pulse followed by a pulse transmitted by the sample. Their separation ΔL is the difference in the op-tical path lengths of the two arms of the interferometer. This beam is sent into a FTIR spectrometer (Biorad FTS-60A). The FTIR uses a Michelson interferometer to ob-tain the field autocorrelation function of the pulse pair by scanning the time delay τ between two copies of the pair. The intensity detected with a Si diode contains interfer-ence fringes whenever τ is such that two pulses overlap. This happens if $\tau = 0$ or if $\tau = \pm \Delta L/c$, with c the speed of light. Near $\tau = 0$ the sample pulse overlaps with its own copy and so does the reference pulse. The measured function is then the sum of the field autocorrelations of the two pulses. Near $\tau = \pm \Delta L/c$ one copy of the sample pulse overlaps with one copy of the reference pulse. This produces the cross correlation function of the two fields, which contains both *spectral* and *phase* information of the pulse transport through the sample.

A typical measurement is shown in Fig. 1. Because the interferograms are symmetric, only the part where $\tau > 0$ is shown. In the lower interferogram the sample beam passed through the glycerol but not through the crystal. The cross correlation function appears at a delay of 1.75 ps, introduced by the path length difference between the interferometer arms. The cross correlation function is "filled" with fringes (see inset) that correspond to the electromagnetic field oscillations. Translating the crystal into the beam produces the interferogram in the upper part of Fig. 1. The center frequency was chosen slightly below the stop gap and this leads to a number of dramatic changes. The low sample transmissivity close to the stop gap causes an attenuation, cf. Fig. 2(a). A delay $\Delta \tau$ has been induced, and the cross correlation has increased in width and become asymmetric. Close inspection of the oscillations showed that the cross correlation has developed a chirp: oscillations near the tail are slightly faster than near the front. All these changes become less pronounced if the frequency is tuned away from the stop gap.

In Fig. 2(b) the time delays are plotted versus the central frequency of the incoming pulse. $\Delta \tau$ is the time delay introduced by the crystal plus the capillary minus an equal distance of glycerol, and can therefore be negative. For
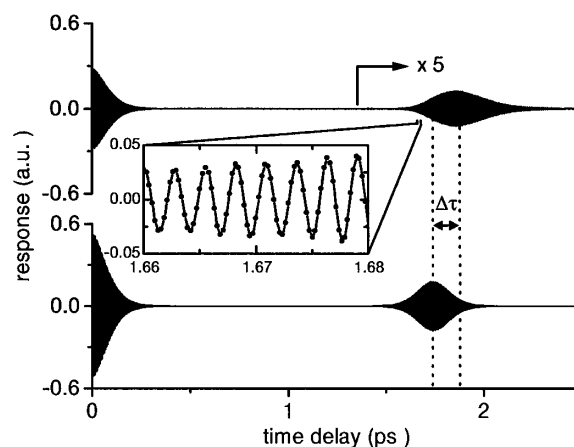

FIG. 1. Interferograms measured with (top) and with-out (bottom) the crystal. Pulses are incident perpendicu-lar to the (111) planes. Their central frequency of $\omega_0 = 2.33 \times 10^{15}$ rad/s (808 nm) is slightly below the L gap. The vertical dotted lines mark the time delay $\Delta \tau$ between the centers of mass of the cross correlations. Data in the upper panel was multiplied by 5 starting from the arrow position. Data are sampled every 0.26 fs so that individual fringes are resolved (inset).

comparison, the sample transmission spectrum, measured in the FTIR with a white light source, is shown in Fig. 2(a). The data clearly demonstrate a large decrease of the group velocity near the edges of the stop gap. The largest time delay measured corresponds to a pulse propagation speed of only about 80% of that far from the gap. This means that the pulse sees an increased effective path length due to multiple reflections in the crystal.

To describe the data in Fig. 2(b) we used the dynamical diffraction theory, originally developed for x-ray diffrac-tion [18]. In its usual formulation, this theory approxi-mates the displacement field in the crystal by the two strongest Fourier components: the incoming and diffracted waves. The theory yields a dispersion relation $\omega(k)$ that can be differentiated to obtain the group velocity. The in-put parameters are the refractive indices of water (1.33) and polystyrene (1.59), as well as the particle diameter (222 nm) and the lattice spacing. The (111) lattice spac-ing is fixed independently by requiring that the predicted location of the stop gap coincides with the center of the transmission minimum. This yielded a value of 284 nm. With all the parameters fixed, the time delay was calcu-lated for a 0.4 mm crystal, and an offset was added to al-low for the capillary and glycerol. The result is shown in Fig. 2(b). The dynamical diffraction theory is seen to describe the data very well. It gives an average refractive index of 1.372 and a relative gap width of 0.032. As an in-dependent check we measured the wavelength-dependent diffraction angle corrected for Snell's law. At 633 nm the crystal was observed to have a diffraction angle of 54.2°, from which we derive a lattice spacing of 286 nm and an average refractive index of 1.366, in agreement with the values above. It has been predicted [21] that crystals with
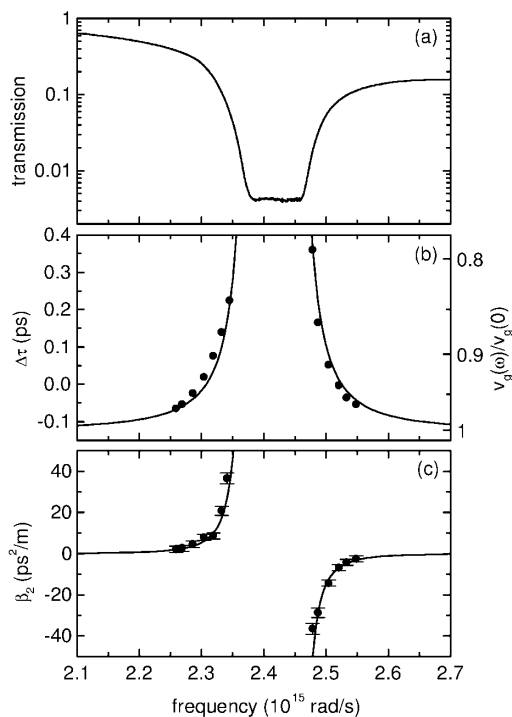
FIG. 2.   (a) Transmission spectrum of the photonic crystal. (b) Measured pulse delay times ($\Delta\tau$, circles) near the L gap versus the central frequency of the incoming pulses. (c) Measured group velocity dispersion parameter (β_2, circles). The lines in (b) and (c) represent the dynamical diffraction theory [18].

high-index spheres in a low-index background are best approximated by expansion of the displacement field as opposed to the electric field. Indeed, an analogous theory that keeps the two strongest components of the *electric* field [22] did not describe the data as well. Even though the measurements explore only one set of lattice planes, one-dimensional models do not describe the data as well as the 3D dynamical diffraction theory. The best mapping of the real 3D crystal onto a 1D multilayer stack was obtained with the model of Lidorikis *et al.* [23], which also needs no adjustable parameters. This model gives a reasonable correspondence to the data, but the gap width is off by 40%, which then results in differences with the measured delay times.

The arrival time of the pulses was taken here as the center of mass of the cross correlation function. However, if the frequency comes very close to the band edges the transmitted pulse shape is distorted (as in Fig. 1). It then becomes uncertain how to take the time delay so that it corresponds best to the group velocity. For example, taking the time delay at the maximum of the cross correlation makes the $\Delta\tau$ values closest to the divergence come out 0.06 ps smaller, while data farther away are unaffected. This does not change the qualitative behavior displayed by Fig. 2(b), but it does demonstrate the well-known fact that the pulse propagation velocity becomes different from the group velocity whenever significant pulse reshaping takes place [24,25].

A quantity that is unambiguous when pulse reshaping takes place is the group velocity *dispersion*, because it quantifies the relative phase shift of the frequencies in the wave packet, which does not depend on its overall shape. The phase information is contained in the fringes of the cross correlation function [17,26]

$$C(\tau) = \frac{1}{\Delta T} \int_{-\Delta T/2}^{\Delta T/2} E_{\text{ref}}^*(t) E_{\text{sample}}(t - \tau)\, dt. \quad (1)$$

The laser's repetition time ΔT is much longer than the pulse duration. The complex Fourier transform of C can be divided by the same object measured without the sample C_0 to obtain the complex transmission function of the sample $H(\omega)$:

$$\frac{C(\omega)}{C_0(\omega)} = \frac{E_{\text{sample}}(\omega)}{E_{\text{ref}}(\omega)} \equiv H(\omega). \quad (2)$$

This procedure also divides out the small dispersion of the lenses and the glycerol. The modulus and argument of $H(\omega)$ are the field transmissivity $t(\omega)$ and the relative phases of the frequencies in the pulse. We can write

$$H(\omega) = t(\omega)e^{ik(\omega)L}, \quad (3)$$

where, for a crystal with length L, the phase shift is governed by the Bloch wave vector k. Thus, from a single interferogram we obtain the dispersion relation over the frequency range covered by the pulse bandwidth. Its deviation from linearity is analyzed with a Taylor expansion around the pulse's central frequency ω_0:

$$k(\omega) = k(\omega_0) + \beta_1(\omega - \omega_0)$$
$$+ \tfrac{1}{2}\beta_2(\omega - \omega_0)^2 + \dots. \quad (4)$$

The coefficients $\beta_1 = (dk/d\omega)|_{\omega_0}$ and $\beta_2 = (d^2k/d\omega^2)|_{\omega_0}$ are the inverse group velocity and the group velocity dispersion, respectively.

This procedure is illustrated using the cross correlations in Fig. 1. The (normalized) moduli of their Fourier transforms are shown in Fig. 3. The spectrum of the sample has become slightly asymmetric and its maximum is shifted to lower frequency. This is because, although the sample spectrum is attenuated as a whole, the frequencies closer to the stop gap are attenuated more strongly. Also shown is the argument of $H(\omega)$ with a term linear in frequency subtracted to make the curvature visible. The parabolic shape reflects the fact that higher frequencies have propagated more slowly through the crystal than lower frequencies. A slight asymmetry can also be seen, indicating that the GVD increases towards higher frequencies, where the stop gap is located. Both the dispersion-induced chirp and the asymmetry of the transmitted spectrum contribute to the asymmetric pulse broadening that was observed in Fig. 1.

The GVD parameter β_2 and cubic coefficient β_3 were obtained from a polynomial fit of the argument of $H(\omega)$. The β_2 values are shown in Fig. 2(c). If the pulse frequency comes to within a few percent of the band
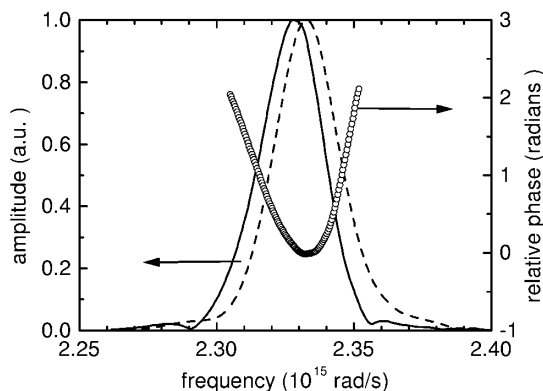
FIG. 3. Moduli of the complex Fourier transforms of the cross correlation functions of Fig. 1. The sample spectrum (solid line) has become slightly asymmetric and has shifted to a lower frequency than that without sample (dashed line). Both spectra were normalized to unity (the sample spectrum was 6 times weaker). The phase of the complex transmission function $H(\omega)$ is the difference between the arguments of the two Fourier transforms (open circles).

edges the GVD diverges. The measured values are 2 to 3 orders of magnitude larger than well-known values for ordinary glass. At the high-frequency side of the stop gap we find a branch of anomalous dispersion. This is quickly recognized in an experiment because the argument of $H(\omega)$ becomes a parabola pointing up instead of down. The cubic coefficient (not shown) was found to be positive again on both sides of the gap. The line in Fig. 2(c) is β_2 calculated from the dynamical diffraction theory by taking the second derivative of k with respect to ω, using the same parameter values as before. Again, the data are described remarkably well by this theory. In analogy to electrons in semiconductors, our measurements can be interpreted as large effects on the effective photon mass, which is negative below and positive above the gap.

The time delay and the GVD result from independent measurements, but in order to be consistent they must be related as $d(\Delta t)/d\omega = d(L/v_g)/d\omega = L\beta_2$. It was verified that β_2 calculated from the time delays by numerical differentiation indeed agrees with the measured values within experimental accuracy.

It is interesting to note that the measured dispersive effects are equally pronounced on both sides of the stop gap. Typical photonic crystals, in contrast, generally transmit much less on the high-frequency side of the gap than on the low-frequency side [see Fig. 2(a)]. This is usually attributed to lattice defects, which scatter higher frequencies more efficiently. These defects, therefore, do not affect the group velocity and GVD.

The large dispersive effects of the band edges that we measured make it possible to locate these edges very accurately. Although the low transmission did not permit measurements inside the stop gaps (but these may be done in reflection), the group velocity dispersion should rapidly decrease to zero there because the real part of k is constant. Thus we predict that, given a pulse frequency

inside a stop gap, rotating the crystal will result in a large dispersion only close to a band edge, and should give no dispersion at all angles if the crystal has a complete photonic band gap.

[1] *Photonic Band Gap Materials,* edited by C. M. Soukoulis, NATO ASI Ser. E, Vol. 315 (Kluwer, Dordrecht, 1996).
[2] E. Yablonovitch, Phys. Rev. Lett. **58**, 2059 (1987).
[3] S. John, Phys. Rev. Lett. **58**, 2486 (1987).
[4] W. M. Robertson, G. Arjavalingam, R. D. Meade, K. D. Brommer, A. M. Rappe, and J. D. Joannopoulos, Phys. Rev. Lett. **68**, 2023 (1992).
[5] E. Özbay, A. Abeyta, G. Tuttle, M. Tringides, R. Biswas, C. T. Chan, C. M. Soukoulis, and K. M. Ho, Phys. Rev. B **50**, 1945 (1994).
[6] C. J. Herbert and M. S. Malcuit, Opt. Lett. **18**, 1783 (1993).
[7] I. I. Tarhan and G. H. Watson, Phys. Rev. Lett. **76**, 315 (1996).
[8] W. L. Vos, R. Sprik, A. van Blaaderen, A. Imhof, A. Lagendijk, and G. H. Wegdam, Phys. Rev. B **53**, 16 231 (1996); *ibid.* **55**, 1903(E) (1997).
[9] I. I. Tarhan, M. P. Zinkin, and G. H. Watson, Opt. Lett. **20**, 1571 (1995).
[10] B. T. Rosner, G. J. Schneider, and G. H. Watson, J. Opt. Soc. Am. B **15**, 2654 (1998).
[11] A. M. Steinberg, P. G. Kwiat, and R. Y. Chiao, Phys. Rev. Lett. **71**, 708 (1993).
[12] C. Spielmann, R. Szipöcs, A. Stingl, and F. Krausz, Phys. Rev. Lett. **73**, 2308 (1994).
[13] M. Scalora *et al.,* Phys. Rev. E **54**, R1078 (1996).
[14] Y. A. Vlasov *et al.,* Phys. Rev. E **60**, 1030 (1999).
[15] S. John and N. Aközbek, Phys. Rev. Lett. **71**, 1168 (1993).
[16] M. Scalora, J. P. Dowling, C. M. Bowden, and M. J. Bloemer, Phys. Rev. Lett. **73**, 1368 (1994).
[17] R. H. J. Kop and R. Sprik, Rev. Sci. Instrum. **66**, 5459 (1995).
[18] R. W. James, *The Optical Principles of the Diffraction of X-Rays* (Bell & Hyman, London, 1962).
[19] M. Beck, I. A. Walmsley, and J. D. Kafka, IEEE J. Quantum Electron. **27**, 2074 (1991).
[20] W. L. Vos, M. Megens, C. M. van Kats, and P. Bösecke, Langmuir **13**, 6004 (1997).
[21] H. S. Sözüer, J. W. Haus, and R. Inguva, Phys. Rev. B **45**, 13 962 (1992).
[22] K. W. K. Shung and Y. C. Tsai, Phys. Rev. B **48**, 11 265 (1993).
[23] E. Lidorikis, Q. Li, and C. M. Soukoulis, Phys. Rev. E **55**, 3613 (1997).
[24] L. Brillouin, *Wave Propagation and Group Velocity* (Academic, New York, 1960).
[25] S. Chu and S. Wong, Phys. Rev. Lett. **48**, 738 (1982), and references therein.
[26] R. H. J. Kop, P. de Vries, R. Sprik, and A. Lagendijk, Opt. Commun. **138**, 118 (1997).